



This is a repository copy of *Process design, operation and economic evaluation of compressed air energy storage (CAES) for wind power through modelling and simulation*.

White Rose Research Online URL for this paper:
<http://eprints.whiterose.ac.uk/146677/>

Version: Accepted Version

Article:

Meng, H., Wang, M. orcid.org/0000-0001-9752-270X, Olumayegun, O. orcid.org/0000-0003-3801-6385 et al. (2 more authors) (2019) Process design, operation and economic evaluation of compressed air energy storage (CAES) for wind power through modelling and simulation. *Renewable Energy*, 136. pp. 923-936. ISSN 0960-1481

<https://doi.org/10.1016/j.renene.2019.01.043>

Article available under the terms of the CC-BY-NC-ND licence
(<https://creativecommons.org/licenses/by-nc-nd/4.0/>).

Reuse

This article is distributed under the terms of the Creative Commons Attribution-NonCommercial-NoDerivs (CC BY-NC-ND) licence. This licence only allows you to download this work and share it with others as long as you credit the authors, but you can't change the article in any way or use it commercially. More information and the full terms of the licence here: <https://creativecommons.org/licenses/>

Takedown

If you consider content in White Rose Research Online to be in breach of UK law, please notify us by emailing eprints@whiterose.ac.uk including the URL of the record and the reason for the withdrawal request.



eprints@whiterose.ac.uk
<https://eprints.whiterose.ac.uk/>

Process design, operation and economic evaluation of compressed air energy storage (CAES) for wind power through modelling and simulation

Hui Meng^a, Meihong Wang^{*,a}, Olumide Olumayegun^a, Xiaobo Luo^a, Xiaoyan Liu^b

- a. Department of Chemical and Biological Engineering, Faculty of Engineering, The University of Sheffield, Mappin Street, Sheffield, S1 3JD, UK.
- b. State Key Laboratory of Chemical Engineering, Department of Chemical Engineering, Tsinghua University, Beijing, 100084, China.

Abstract

Compressed air energy storage (CAES) could play an important role in balancing electricity supply and demand when linked with fluctuating wind power. This study aims to investigate design and operation of a CAES system for wind power at design and off-design conditions through process simulation. Improved steady-state models for compressors, turbines and the CAES system for wind power were developed in Aspen Plus[®] and validated. A pseudo-dynamic model for cavern was developed in Excel. Compressor and turbine characteristic curves were used in model development for process analysis. In the off-design analysis, it was found that the CAES system for wind power at variable shaft speed mode utilise more excess wind energy (49.25MWh), store more compressed air (51.55×10^3 kg), generate more electricity (76.00MWh) and provide longer discharging time than that at constant shaft speed mode. Economic evaluation based on levelized cost of electricity (LCOE) was performed using Aspen Process Economic Analyser[®], it was found that LCOE for the CAES system for wind power at variable shaft speed mode is lower than that at constant shaft speed mode. Research presented in this paper hopes to shed light on design and operation of the CAES system for wind power and cost reduction.

Keywords:

Compressed air energy storage (CAES), Wind power, Off-design analysis, Process simulation, Process integration, Economic evaluation

Nomenclatures

W_t	The output power of Turbine (kWh)
W_e	Electrical energy taken from wind farm for driving the compressors (kWh)
E_f	Fuel input energy (kWh)
η_{sys}	System electric efficiency
η_{eff_1}	Round-trip efficiency of the CAES system
η_{eff_2}	Round-trip efficiency of the CAES system with system electric efficiency
n	CAES plant lifetime
i	Discount rate
r	Reference CAES system condition
s	Simulation result
re	Relative error
P	The pressure of the cavern (Pa)
V	The volume of the cavern (m ³)
m_{Air}	The mass of the compressed air injected into the cavern (kg)
M_{Air}	The molar mass of the air (kg/kmol)
R	Ideal gas constant (J K ⁻¹ mol ⁻¹)
T	The temperature in the cavern (K)

Abbreviations

CAES	Compressed air energy storage
LCOE	Levelized cost of electricity
LPC	Low-pressure compressor
HPC	High-pressure compressor
LPT	Low-pressure turbine
HPT	High-pressure turbine
APEA	Aspen Process Economic Analyser®
TAC	Total annual cost
ACAPEX	Annualised capital expenditure
FOPEX	Fixed operation expenditure
VOPEX	Variable operational expenditure
CRF	Capital recovery factor
CAPEX	Capital expenditure

1. Introduction

The use of renewable energies such as wind and solar power continues to increase in many countries since greenhouse gas emissions from conventional power plants have resulted in severe environmental problems [1,2]. The wind power generation reached 3% (i.e. 435GW) of global electricity production in 2015 and it is expected to increase from 11.6% (3599 TWh) in 2030 to 14.8% (6145 TWh) in 2050 [3,4]. The increasing utilisation of renewable energy could lead to a new challenge - the imbalance between electricity generation and demand. This is due to the intermittent nature of renewable energy, whose output mainly depends on local environmental conditions and unpredictable weather [1,5]. Wind power as one of the major renewable energy sources is also intermittent. Several studies have suggested ways to overcome this problem. One such solution is the application of energy storage technologies, which can be integrated with wind power to improve the stability and reliability of wind power [6–9]. Energy storage technologies can play a vital role in load levelling [6,10], peak shaving [6,10,11], renewable energy integration [10,11] and power quality improvement [1].

Energy storage technologies include pumped hydro storage (PHS), compressed air energy storage (CAES), flywheels, batteries, superconducting magnetic energy storage and supercapacitors [6,11–16]. Currently, only PHS and CAES can be implemented at grid-scale capacity of more than 100 MWe. The mature PHS has been widely implemented around the world. However, the PHS is limited by the geographical requirement as it requires two large reservoirs at different elevations to store water. On the other hand, the CAES only requires an underground cavern to store the compressed air [6,15,17–19]. Furthermore, the application potentials of a CAES system include: peak shaving, load levelling, energy management, renewable energy integration and standby power [6,10,20]. Therefore, CAES as one grid-scale energy storage technology can be an attractive and a promising option to mitigate the intermittency problem of large-scale wind power generation [4,8]. Figure 1 shows that CAES system can be used to transfer excess or off-peak wind electricity to high demand periods. For example, from 1 am to 4 am and from 6 am to 10 am, the external electricity demand is low, the off-peak excess electricity will drive compressor and the cavern pressure increases. From 11 am to 13 pm, the external electricity demand becomes higher, the stored air will be expanded to drive turbines for electricity generation.

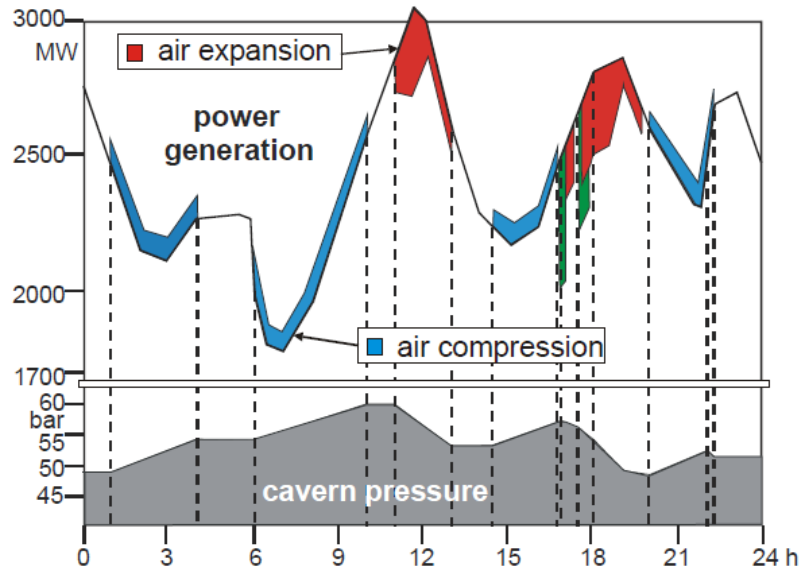


Figure 1. Operation of the CAES system integrated with wind power within 24 hours [21].

To date, two commercial CAES plants have been operated. The Huntorf CAES plant in Germany started operation in 1978 and has a rated power of 290 MWe with more than 2 hours of discharging operation [6,10,21]. The second plant, the McIntosh CAES plant in the USA, started operation in 1991 and has a rated power of 110MWe with up to 26 hours discharging duration [6,16,20]. It uses a recuperator to recover waste heat from the turbine exhaust to preheat the compressed air. This improves the round-trip efficiency of the McIntosh CAES plant to 54% which is higher than the round-trip efficiency of the Huntorf CAES plant (around 42 %). Fuel consumption is also reduced by about 25% [20]. In 2016, an advanced CAES system with a rated power 10 MWe was constructed in China. This plant is mainly for research and demonstration of wide-load compressors, high-load turbines and heat exchangers for the CAES system [22].

In recent years, many researchers have focused on the investigation CAES system integrated with renewable energy sources (e.g. wind power and photovoltaic power) to overcome the intermittency problem of renewable energy. Zhang et al. [23] developed a model for an adiabatic CAES system with variable configuration (VC-ACAES) integrated with wind farm. It was found that when wind farm was integrated with the VC-ACAES, the fluctuating wind power (average 21.05 MW, up to 49.5 MW) can be stabilized to a steady power generation of 18.5 MW and the wind power utilization coefficient was increased from 26.29% to 70.62%. Simpure et al. [24] suggested an integrated system of the CAES with photovoltaic power to overcome the intermittency problem of photovoltaic electricity in Reunion, France. The limitation is that the integrated system was not connected to the grid network due to the limitation of the location condition. A model for the integrated system was developed to evaluate its feasibility. The process analysis by simulation study on key parameters of

the system was investigated and the simulation results including the round-trip efficiency, the load coverage ratio and the energies were discussed for achieving better system performance. Economic evaluation of CAES system integrated with wind power to curtail intermittency problem has also been investigated [25,26]. Cavallo [27] concluded that a CAES system integrated with wind power can be a viable strategy for the wind farm. The operation, control and management strategies of CAES system integrated with wind power have been proposed using a mathematical model [28–32]. Briola et al. [33] developed a quasi-stationary mathematical model of a CAES system and investigated the characteristic curves of the compressors and turbines for the purpose of performance analysis.

Sun et al. [34] presented a unidirectional hybrid CAES-wind turbine system using a scroll expander to drive the shaft of wind turbine through a mechanical transmission system for smoothing the wind power output. Krupke et al. [35] showed a bidirectional hybrid CAES-wind turbine system, a single stage of turbomachinery (e.g. scroll-compressor or scroll-expander) of the CAES system connects to the shaft of the wind turbine for smoothing the fluctuating wind power. However, the experimental study for the efficiency of this integrated system was only 37% due to the loss of massive heat. The difference between these two aforementioned hybrid systems is that the bidirectional hybrid system not only enables the turbomachinery of a CAES system to be connected to the wind turbines for smoothing the fluctuating wind power, but also the turbomachinery can serve as a compressor or expander for servicing the charging and discharging processes of a CAES system [35].

Li et al. [36] proposed a mathematical model of a CAES system integrated with a vertical axis wind turbine (VAWT). It was concluded that the integrated system with the control strategy enables the round-trip efficiency to increase by 5.21% and the integrated system can overcome the fluctuating power output from VAWT and generate 30kW stable power. Ibrahim et al. [37] studied the CAES system integrated with wind-diesel hybrid systems to optimise its cost and performance. The proposed design of the integrated system requires repowering of current facilities including an increase of power output, engine lifetime and efficiency for reducing 20-25% fossil fuel consumption and greenhouse gas emissions, also saving the cost of system maintenance and replacement [37]. Marano et al. [28] investigated a dynamic model for a hybrid system of a wind farm, a photovoltaic system and a CAES system on a daily cycle for energy, economics and environmental impacts. This study was also to determine the optimal management strategy with the target to maximise the profits and minimise the cost. It was found that the hybrid system can improve the economic viability of renewable energy sources. Moreover, the operating cost can be reduced by about 80% with respect to the conventional solution and the CO₂ emissions can be reduced by 74%.

Most of the mathematical models and simulations of CAES systems reported in the literature were for system analysis at design condition. The off-design performance of a CAES system for wind power is yet to be investigated and most of the models did not include the characteristic curves of the compressors and turbines. Hence, the models could not accurately predict operating points during charging and discharging processes of the CAES system in the context of changing wind power. In this paper, the model of the CAES system in the context of wind power allows accurate determination of different operation points (design and off-design) for the compressors and turbines based on the characteristic curves. This paper aims to study operation strategies, process investigation and economic evaluation of a CAES system for wind power at both design and off-design conditions. To achieve the aim, the following objectives have been identified:

- To develop and validate improved models of the CAES system:
 - Improved models for the compressors and turbines based on their characteristic curves
 - Pseudo-dynamic model for the cavern of the CAES system
 - Improved model of the entire CAES system for wind power
- To perform process analysis of the CAES system for wind power at design and off-design conditions involving the different modes: constant and variable shaft speed modes.
- To perform economic evaluation of the CAES system for wind power at design and off-design conditions.

The novel contributions of this paper include:

- Improved steady-state models were developed for compressors and turbines of the CAES system based on characteristic curves in Aspen Plus[®] and Fortran and a pseudo-dynamic model for the cavern was developed in Excel.
- Improved model for the CAES system in the context of wind power at design and off-design conditions was developed.
- Different operation strategies for the CAES system in the context of wind power were proposed for different wind power output conditions (above or below 110 MWe).
- Process analysis of the CAES system for wind power at design and off-design conditions was investigated, also two different modes (constant and variable shaft speed modes) at off-design conditions were evaluated.
- Economic evaluation for the CAES system for wind power at design and off-design conditions was carried out using Aspen Process Economic Analyser[®] (APEA).

2. Process description of the CAES system integrated with wind power

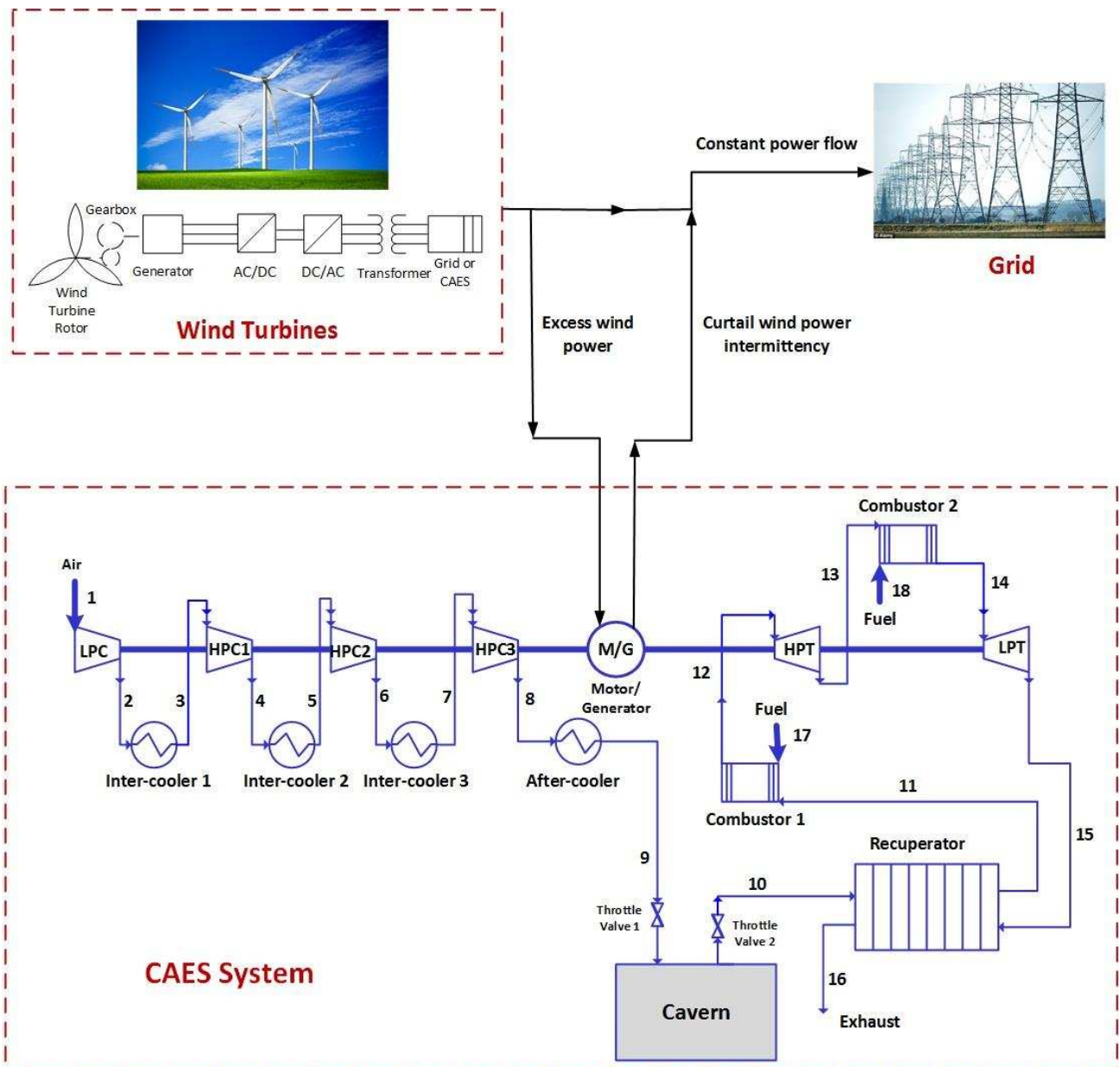


Figure 2. The schematic diagram of the CAES system integrated with wind turbines

The integrated system (refer to Figure 2) includes wind turbines, a CAES system and the electricity grid. Under normal circumstance, the wind farm will transmit all the electric power generated directly to the electricity grid. However, if the wind power output is more than the grid demand, the excess electricity can be utilised to drive the compressors for compressing air in the charging process of the CAES system. The compressed air is injected into an underground cavern at high pressure. When the output power from the wind farm is below grid demand, the stored compressed air can be expanded in the turbines to generate electricity to balance the insufficient wind power output during the discharging process of the CAES system. With a recuperator, the compressed air extracted from the

cavern is preheated with the waste heat from the turbine exhaust to improve the round-trip efficiency of the CAES system. Then, the preheated air passes into the combustor, where it is mixed with fuel and combusted. The high-temperature combustion product is expanded in the turbines to generate electricity [10,19,20]. Therefore, one advantage of integrating CAES system with wind power is that the CAES system can be used to curtail the intermittency of wind power by matching the integrated system output with the grid power demand.

A combination of a low-pressure axial compressor, three high-pressure centrifugal compressors and gas turbines were used in Huntorf CAES plant [38–40]. In this study, the outlet pressure of the compression process of the CAES system can reach over 70 bar, so multi-stage compressors with inter-cooling will be implemented. There are four compressors implemented in the charging process of the CAES system: an axial LPC and three centrifugal HPC. Axial compressors are typically used for applications with low differential pressure (head) requirements, high volume air flow rate and higher efficiency (~85%), but the big weight, complex structure and high starting power requirements of the axial compressors are drawbacks [41]. A wide range of pressure rise (6 bar to 70 bar) is required after the first stage of compression. High rotational speed and large impeller size will be needed to achieve such a wide range of pressure rise. However, the maximum allowable speed will be limited by the strength of the structural material of the impeller blades and sonic velocity of the gas. As a result, the limitation on maximum achievable pressure rise can be overcome using high shaft speed centrifugal compressors, which is able to compress the gas to desirable pressure using multiple stages of centrifugal compressors operating in series [41]. It is noticed that the wind speed varies randomly over a wide range, which results in wind power output fluctuating in large magnitude. The operational range of CAES system under off-design condition could be limited by surge margin and choke margin of the centrifugal and axial compressors [23].

In the discharging process, there are two turbines HPT and LPT implemented for two expansion stages. The gas inlet condition of 43 bar and 550 °C for the HPT is a common feature of the steam turbine construction [40]. The steam turbine can work at temperatures between 500 and 650 °C and high, medium and low pressure and the general gas turbine was not compatible with the expansion pressure range from 43 bar to 11 bar [42,43]. Therefore, the HPT is designed based on the engineering principle of the steam turbine [40]. The LPT is designed based on the engineering principle of gas turbine with hot combustion gases available at high temperature up to 1500 °C and a pressure drop from 11 bar to 1 bar at turbine exit [40,42].

3. Operation strategies and characteristic curves for compressors and turbines

3.1 Operation strategies of the CAES system integrated with wind power

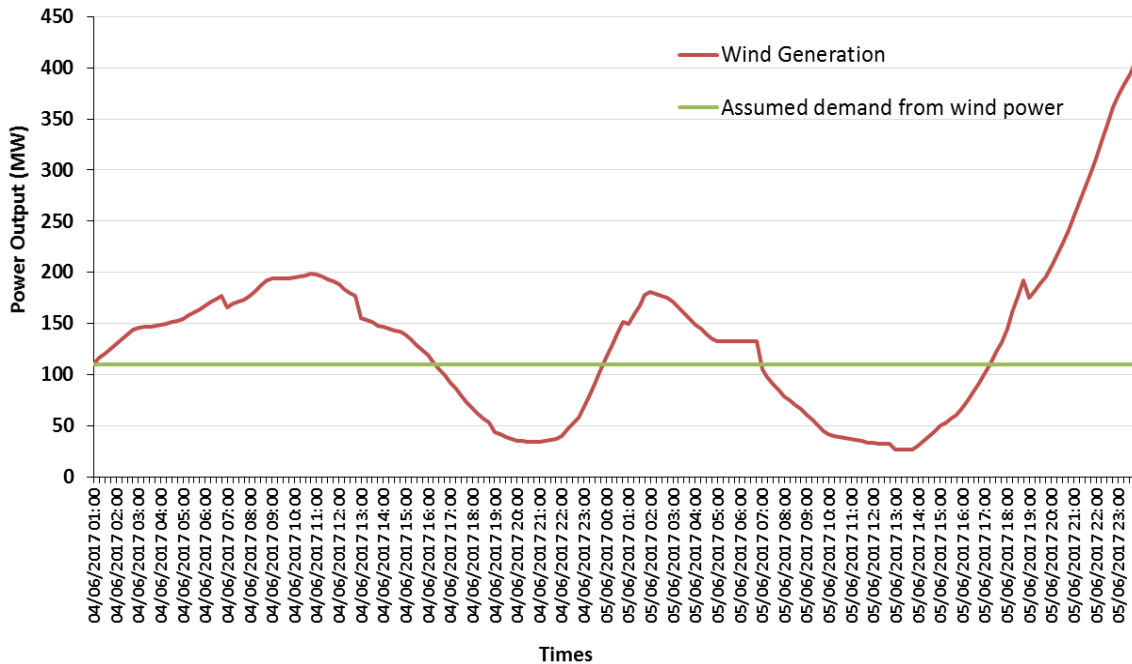


Figure 3. Wind power output in Northern Ireland over a 48-hour period [44].

The wind power output in Northern Ireland (including onshore and offshore wind farms) over a 48-hour period is shown in Figure 3. The power output is seen to fluctuate between 30 MWe and 400 MWe during this period. For the purpose of this study, it is assumed that the wind power required to be supplied to the electricity grid is 110 MWe at all time (as shown with the solid green line in Figure 3). The operation strategies of the integrated system can be summarised as:

- Wind power output above 110 MWe (e.g. from 01:00 to 16:00 in Figure 3): 110 MW of electricity is supplied to the grid and the excess electricity is used in the CAES system for storing energy in the form of compressed air;
- Wind power output below 110 MWe (e.g. from 16:00 to 24:00 in Figure 3): The compressed air in the CAES system is expanded to generate electricity to balance the wind power output
- Wind power output plus the CAES system power output below 110 MWe: It is assumed that the electricity produced from other power plants (e.g. a conventional power plant) will cover the imbalance [45].

3.2 Characteristic curves for the compressors and turbines of the CAES system

Figures 4 and 5 show the characteristic curves for the compressors and the turbines of the CAES system [33]. They will be used to obtain their corresponding performance at different operating points

for model development and simulation. Figures 4 (a) and (b) present the characteristic curves of the LPC (the axial compressor) and HPC (the centrifuge compressors), and the relationship between mass flow rate and pressure ratio. Figures 5 (a) and (b) present the characteristic curves of the LPT and HPT, and the relationship between pressure ratio and mass flow rate. Different shaft speeds of the compressors or the turbines were normalised as the different dimensionless velocities. For example, when the dimensionless velocity equals to 1 ($v = 1$), the CAES system will operate at design shaft speed. When the dimensionless velocity is above or below 1 ($v > 1$ or $v < 1$), the CAES system will operate at off-design shaft speed. The optimal efficiency lines in Figures 4 and 5 show the optimal efficiencies operated at different shaft speeds for the compressors and turbines of the CAES system.

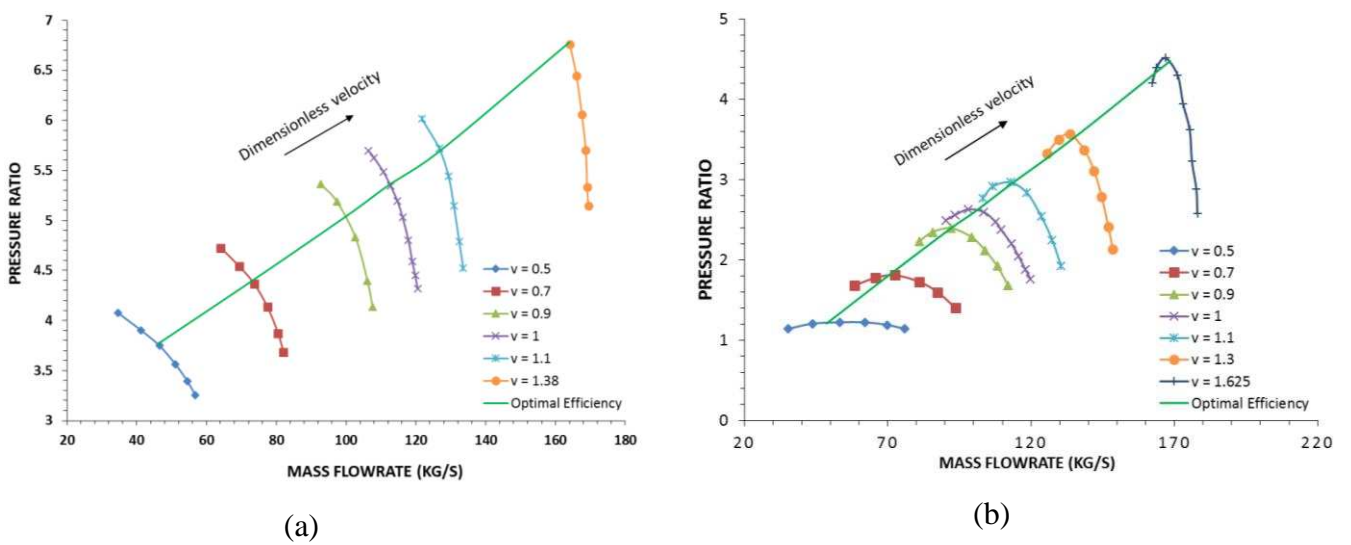


Figure 4. Characteristics curves of (a) LPC and (b) HPC of the CAES system [33]

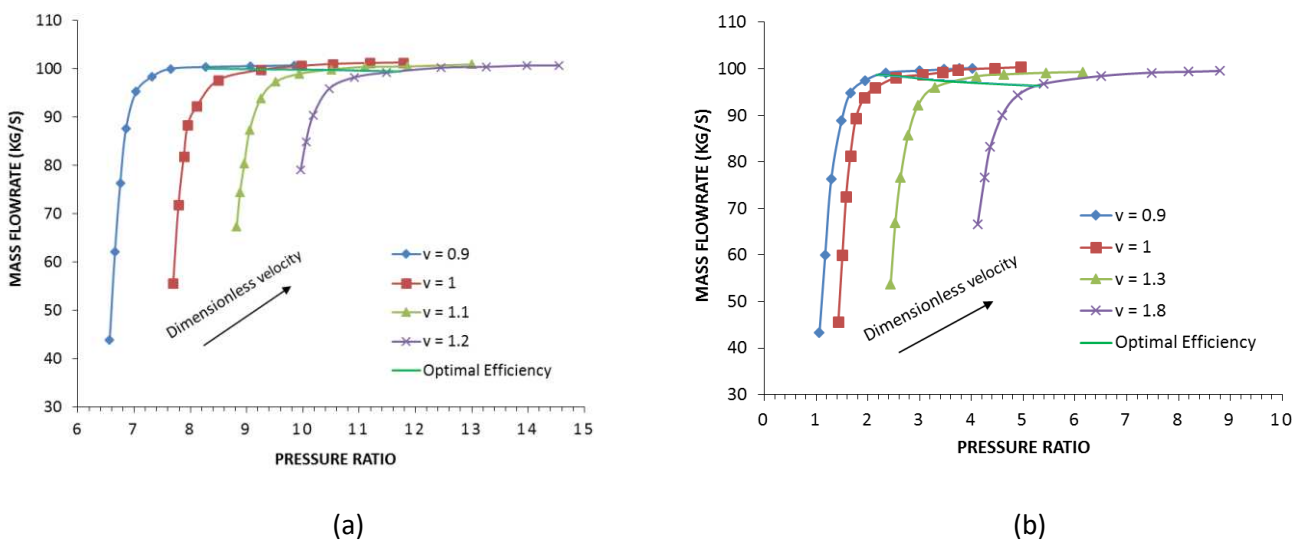


Figure 5. Characteristics curves of (a) LPT and (b) HPT of the CAES system [33]

4. Model development, model validation and performance criteria of the CAES system

4.1 Model development

4.1.1 Development of improved models Compressors and turbines

The performance characteristic curves of the compressors shown in Figure 4 and the turbines shown in Figure 5 were used to obtain their corresponding performance at different operating points. These operation points from performance curves were entered into the Aspen Plus® models of the compressors and turbines to simulate their off-design performance through Performance Rating. As for the compressor models, there are several characteristic curves at different shaft speeds for two types of compressors in Figure 4, The parameters including pressure ratio and mass flowrate were chosen in the Performance and Flow Variables. The data at different operating points can be filled in the curve data form. As for the turbine models, there are four characteristic curves at different shaft speeds for the two turbines in Figure 5. The procedures of model development for the turbines are almost the same as that of the compressors. As for the optimal efficiency at off-design conditions, the model of the optimal efficiency for different shaft speed curves can be developed in Fortran which can be connected to the Aspen Plus®. The results will be carried out by Fortran calculator and used for the Aspen Plus® model.

4.1.2 Pseudo-dynamic model for cavern of CAES system

The model of the cavern was developed in Excel as a pseudo-dynamic model as shown in Equation (1) based on the Ideal Gas Law ($PV = nRT$) [46].

$$PV = \frac{m_{Air}}{M_{Air}} \cdot RT \quad (1)$$

A dynamic process varies with time with considerable change in terms of value. A pseudo-dynamic process is also time dependent but change is slow (e.g. the pressure of cavern was changed hourly). The pseudo-dynamic approach enables approximate simulation of various dynamics in accordance with their actual timescales, the accuracy and practicality will be improved [47]. In Figure 6, assuming the cavern pressure changes hourly in this study. During the charging period, the pressure of the cavern will increase with increasing mass of the compressed air injected into the cavern. On the contrary, the pressure of the cavern will decrease when the compressed air expanded during the discharging period. As for the cavern model, during the charging period, the cavern pressure was updated hourly in Excel according to the mass flowrate of the incoming compressed air. Similarly,

during the discharging period, the cavern pressure was also changed hourly according to the air mass flowrate to out of cavern.

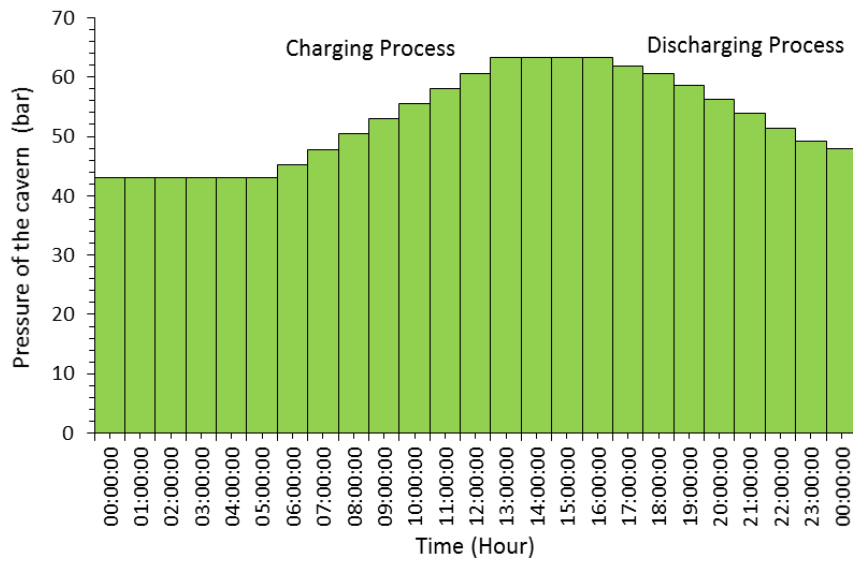


Figure 6. The pressure condition of the carven during charging and discharging processes of the CAES system for wind power.

It is noted that modelling of the cavern was assumed to follow the Ideal Gas Law which relates pressure, temperature, and volume of the ideal gas. However, the Ideal Gas Law is accurate only at relatively low pressures and high temperatures. To account for deviation from the ideal situation, another factor called the gas compressibility factor need to be considered. Therefore, the Non-Ideal Gas Law could become: $PV = Z \cdot nRT$ (Z is the gas compressibility factor, n is number of moles of gas present) [48].

Table 1. Compressibility factor for air [48].

Temperature [K]	Compressibility factor for Air - Z -													
	Pressure [bar absolute]													
	1	5	10	20	40	60	80	100	150	200	250	300	400	500
75	0.005	0.026	0.052	0.104	0.206	0.308	0.409	0.510	0.758	1.013				
80		0.025	0.050	0.100	0.198	0.296	0.393	0.489	0.726	0.959	1.193	1.414		
90	0.976	0.024	0.045	0.094	0.187	0.278	0.369	0.468	0.678	0.893	1.110	1.311	1.716	2.111
100	0.980	0.887	0.045	0.090	0.178	0.264	0.350	0.434	0.639	0.838	1.040	1.223	1.594	1.954
120	0.988	0.937	0.886	0.673	0.178	0.256	0.337	0.413	0.596	0.772	0.953	1.108	1.509	1.737
140	0.993	0.961	0.921	0.830	0.586	0.331	0.374	0.434	0.591	0.770	0.911	1.039	1.320	1.590
160	0.995	0.975	0.949	0.895	0.780	0.660	0.570	0.549	0.634	0.756	0.884	1.011	1.259	1.497
180	0.997	0.983	0.966	0.931	0.863	0.798	0.743	0.708	0.718	0.799	0.900	1.007	1.223	1.436
200	0.998	0.989	0.977	0.954	0.910	0.870	0.837	0.814	0.806	0.855	0.931	1.019	1.205	1.394
250	0.999	0.996	0.991	0.982	0.967	0.955	0.946	0.941	0.945	0.971	1.015	1.070	1.199	1.339
300	1.000	0.999	0.997	0.995	0.992	0.990	0.990	0.993	1.007	1.033	1.067	1.109	1.207	1.316
350	1.000	1.000	1.000	1.001	1.004	1.008	1.012	1.018	1.038	1.064	1.095	1.130	1.212	1.302
400	1.000	1.001	1.003	1.005	1.010	1.016	1.023	1.031	1.053	1.080	1.109	1.141	1.212	1.289
450	1.000	1.002	1.003	1.006	1.013	1.021	1.029	1.037	1.061	1.091	1.118	1.146	1.209	1.278
500	1.000	1.002	1.003	1.007	1.015	1.023	1.032	1.041	1.065	1.091	1.118	1.146	1.205	1.267
600	1.000	1.002	1.004	1.008	1.016	1.025	1.034	1.043	1.068	1.092	1.117	1.143	1.195	1.248
800	1.000	1.002	1.004	1.008	1.016	1.024	1.032	1.041	1.062	1.084	1.106	1.128	1.172	1.215
1000	1.000	1.002	1.004	1.007	1.014	1.022	1.029	1.037	1.056	1.074	1.095	1.113	1.152	1.189

In this study, the regular operating pressure of the cavern is between 43bar and 66bar and the temperature of the compressed air in the cavern is assumed constant at 50°C (323.15K). From summary of compressibility factor for air in Table 1, it was found that there is no much influence on the compressibility factor of the air between 40bar and 70bar at constant temperature of 50°C (323.15K), the compressibility factors of the air are approximately 0.998 (40bar) and 1.000 (70bar) at 325K. Therefore, modelling compressed air in the cavern model can be based on the ideal gas in this paper.

4.1.3 Improved model for the CAES system in the context of wind power

The CAES model was divided into three sections: charging, storage and discharging sections. The main components of the CAES system include compressors, intercoolers, aftercooler, cavern, recuperator, combustors and turbines. Steady-state models for the charging and discharging processes of the CAES system were developed and simulated in Aspen Plus[®] with input parameters based on industrial operation consideration. The improved models for the compressors and turbines were developed based on the characteristic curves in Figures 4 and 5 in Section 3.2 and the details have been described in Section 4.1.1. The model is capable of predicting the components' performance of the CAES system at the design and off-design conditions. The model of the cavern was developed in Excel and the specific description for the model development of the cavern has been given in Section 4.1.2.

The intercoolers and aftercooler were simulated with Heater blocks, which was selected by heat transfer between process stream and cooling utility. The outlet temperature and pressure were required for implementing this block in the CAES model. The combustor was simulated with RGibbs reactor block. The flow rate of air is chosen so as to ensure complete (equilibrium) combustion of the natural gas. The RGibbs block calculates the equilibriums by the Gibbs free energy minimisation thereby avoiding the complicated calculations of reaction stoichiometry and kinetics. This will simplify the required input parameters for the block. Phase equilibrium and chemical equilibrium was selected as the calculation option for the combustors and the required inputs were temperature and heat duty of the combustor. The recuperator was simulated with a HeatX block because two process streams for heat transfer were specified. The flow direction in the recuperator was chosen to be counter-current flow. The selected input parameters and options for exchanger specifications were design option, exchanger duty and minimum temperature approach. PENG-ROB (Standard Peng-Robinson cubic equation of state) method was implemented for the property calculation for the CAES

model [49]. Different components of the CAES system and corresponding blocks in Aspen Plus[®] were summarised in Table 2.

Table 2. Summary of components of the CAES system and corresponding blocks in Aspen Plus[®]

Components of the CAES system	Blocks of the CAES model
Compressors / Turbines	Compr
Intercoolers / Aftercooler	Heater
Combustors	RGibbs
Recuperator	HeatX

4.2 Model validation of the CAES system

The data of the reference CAES system used for model validation was from Briola et al. [33]. The flowsheet of the CAES plant is shown in Figure 7. The reference CAES system conditions (r), simulation results (s) and the relative errors (re) for the compressors and turbines of the CAES system have been summarised in Tables 3 and 4.

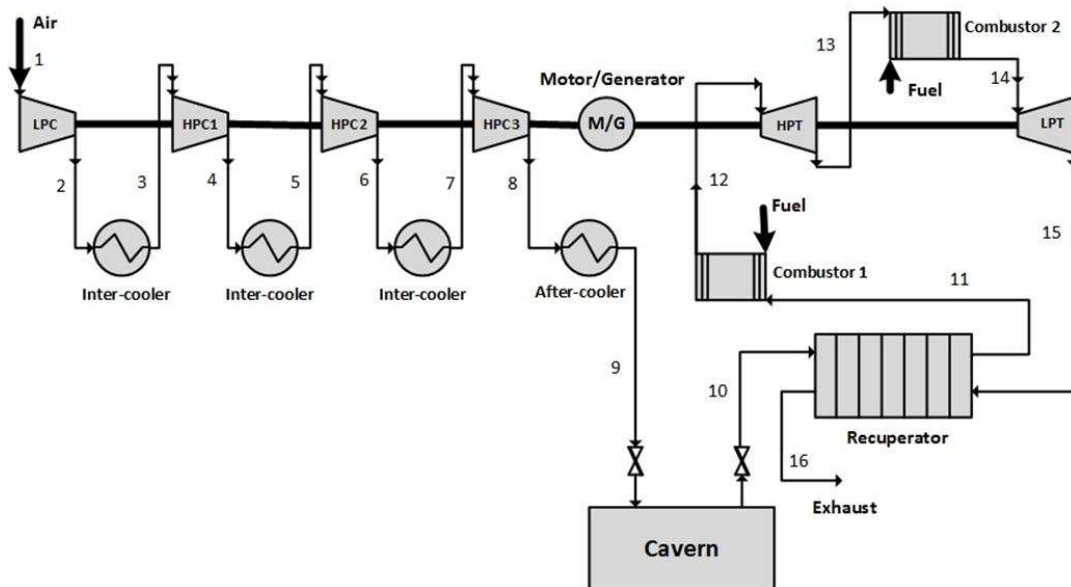


Figure 7. The schematic diagram of the CAES system [33]

In Tables 3 and 4, the simulation results for the compressors and turbines were compared with the reference CAES system condition. The results from process simulation showed that all of the relative errors are less than 2.3% with a good agreement. In addition, a detailed model comparison of a CAES system using Aspen Plus[®] was investigated by Meng et al. [19] and most of the relative errors of the validated model were less than 1%.

Table 3. The reference conditions (r), simulation results (s) and relative errors (re) for compressors

Type	Variables	LPC				HPC 1				HPC 2				HPC 3			
		SN*	r			SN	r			SN	r			SN	r		
Input	P _{in} (bar)	1	1			3	5.8			5	13.1			7	30.7		
	T _{in} (K)	1	283			3	323			5	323			7	323		
	m (kg/s)	1	108			3	108			5	108			7	108		
	Pressure ratio		5.9				2.35				2.37				2.37		
Results	P _{out} (bar)	SN	r	s	re	SN	r	s	re	SN	r	s	re	SN	r	s	re
		2	5.9	5.9	0.0%	4	13.3	13.6	2.2%	6	31.2	31.3	0.03%	8	72	72.8	1.1%
	Power (MW)	Power consumption of LPC				The total power consumption of HPC 1-3											
		r	s	re	r			s			re						
		23.8	24.37	2.3%	35.6			34.93			1.9%						

*SN: Stream Number

Table 4. The reference conditions (r), simulation results (s) and relative errors (re) for turbines

Type	Variables	HPT				LPT			
		SN	r			SN	r		
Input	P _{in} (bar)	12	43			14	11.3		
	T _{in} (K)	12	823			14	1098		
	m (kg/s)	12	410			14	410		
	P _{out} (bar)	13	11.5			15	1		
Results	T _{out} (K)	SN	r	s	re	SN	r	s	re
		13	624	626	0.3%	15	673	681	1.17%
	Power output (MW)	The power output of HPT				The power output of LPT			
		r	s		re	r	s		re
		90	89.24		0.85%	200	201.19		0.59%

4.3 Performance criteria

The CAES system is different from other power plants because two types of input energy are utilised in the system. Electricity is used to drive compressors during the charging period and chemical energy in the fuel is released in the combustor during the discharging period. There are two different Equations (2) & (3) to calculate the round-trip efficiency of the CAES system. A broad overview of these two methods has been described in [19,49–51].

Round-trip efficiency₁

$$\eta_{eff_1} = \frac{W_t}{W_e + E_f} \quad (2)$$

In equation (2), both input energy W_e and E_f are regarded as total input energy and this approach was commonly applied in most of the literatures [19,49–52]. However, this equation could still be challenged because the total input energy includes two different types of energy, electricity to drive compressors and chemical energy from the fuel consumed [50,51].

Round-trip efficiency₂

$$\eta_{eff_2} = \frac{W_t}{W_e + \eta_{sys} \cdot E_f} \quad (3)$$

In Equation (3), the chemical energy contribution of fuel consumed in the combustors is considered due to the combustion system electric efficiency η_{sys} . The value of η_{sys} can be determined by different gas firing conversion power systems. In general, the reference system for electric efficiency could be around 30%. This equation can be regarded as how much electricity is indeed consumed in the system to generate the electricity output of the CAES system.

In this study, Equation (2) using the certain and measurable input energy can be more persuasive for comparison in the round-trip efficiency of the CAES systems because most of the literature adopted it to evaluate the round-trip efficiency. Therefore, this equation will be applied in this paper for the round-trip efficiency of the CAES system.

5. Process investigation of the CAES system for wind power

This section investigates the performance of the CAES system for wind power at the design and off-design conditions.

5.1 Performance investigation of the CAES system for wind power at design condition

In this case, the performance of the CAES system for wind power at design condition will be investigated based on the condition of wind power output in Northern Ireland (refer to Figure 3) and it will be viewed as a base case to compare with the process analysis at off-design conditions. During the charging period, assuming continuous strong wind speed, the wind power output is assumed to be constant at 170 MWe and the power requirement from electricity grid is 110 MWe. Therefore, the 60 MWe electricity from the wind farm will be used by the CAES system. During the discharging period, assuming continuous weak wind speed, the wind power output is assumed to be constant at 34.5 MWe. Thus, the 75.5 MWe electricity generated from the CAES system needs be delivered to the grid. Table 5 lists the wind power condition and input parameters of the CAES system for this case study.

Table 5. The wind power condition and input parameters for the CAES system at design condition

Process parameters	Values
Ambient air temperature (°C)	20
Ambient air pressure (bar)	1.01325
Regular operation pressure of the cavern (bar) [21,40]	43 – 66

Air temperature in the cavern (°C)		50
Air mass flowrate in charging process (kg/s)		108
LPC / HPC ratio		5.6436 / 2.37
HPT / LPT ratio		3.7313 / 10.5263
Air mass flowrate in discharging process (kg/s)		99.60
The inlet pressure of combustor 1 (bar)		43
The inlet temperature of combustor 1 (°C)		50
The inlet temperature of HP / LP turbines (°C)		550 / 825
Exhaust gas temperature (°C)		110
Wind power to compressors (Motor)	Rated power (MW)	60
	Frequency (Hz)	50
	Voltage (kV)	21
	Speed (min ⁻¹)	3000

Some assumptions about the CAES system for wind power are given as follows:

- The pressure drops in the intercoolers and aftercooler are assumed to be 1.5% of the inlet pressure [33].
- The pressure drops of the two combustors are 2% of the inlet pressure [33].
- The fuel used in the CAES discharging process is pure methane.
- The isentropic efficiencies of the compressors and turbines are assumed to be 84% and 90% respectively [33,53].
- The volume of the cavern is assumed to be 140,000 m³.
- The temperature of the compressed air in the cavern is assumed constant at 50 °C.

Simulation results of the CAES system for wind power based on the aforementioned parameters and assumptions are shown in Tables 6 and 7. Table 6 shows the values of the stream variable at each point in the system (refer to Figure 2 for the stream numbering). The simulation results of performance of the system is summarised in Table 7. The total charging electricity of all compressors is 60MW and total discharging electricity output by the turbines is around 75.5MW. The fuel consumed to preheat the compressed air is 83.65MJ/s during the discharging process. The charging time (around 8.94 hours) and discharging time (around 9.70 hours) were calculated by the Equation (1) of the pseudo-dynamic model of the cavern in Section 4.1.2. The round-trip efficiency of the CAES system at design condition is 54.34%. This is around 12.34% higher than round-trip efficiency

of the Huntorf CAES plant (about 42%) due to the use of a recuperator to recover waste heat from the LPT exhaust to preheat the compressed air during the discharging operation.

Table 6. The simulation results of the CAES system for wind power at design condition

Stream Numbers	Pressure (bar)	Temperature (°C)	Flowrate (kg/s)
1	1.01325	20.00	108.00
2	5.72	237.01	108.00
3	5.63	50.00	108.00
4	13.35	155.21	108.00
5	13.15	50.00	108.00
6	31.16	155.32	108.00
7	30.70	50.00	108.00
8	72.57	155.40	108.00
9	71.66	50.00	108.00
10	43.00	50.00	99.60
11	43.00	334.11	99.60
12	42.14	550.00	100.09
13	11.29	332.56	100.09
14	11.06	825.00	101.27
15	1.05	384.90	101.27
16	1.05	110.00	101.27

Table 7. The simulation results of performance of the CAES system for wind power at design condition

Output variables	Values
Total charging electricity of the compressors (MW)	60.00
Total output electricity (MW)	75.50
Total fuel consumption (MJ/s)	83.65
Charging time (Hours)	8.94
Discharging time (Hours)	9.70
Round-trip efficiency (%)	54.34

5.2 Process analysis of the CAES system for wind power at off-design conditions

It is difficult to maintain a steady operation (e.g. constant design condition) for the CAES system in the context of wind power due to the fluctuating wind power output and the changing electricity

output of the CAES system. Thus, the CAES system for wind power would mostly be operated at off-design conditions during the periods of charging and discharging operation. In the off-design analysis, two operation modes will be investigated including constant shaft speed mode and variable shaft speed mode of the compressors. In both cases, the turbines' speed will be maintained at the grid synchronous speed of 3000 rpm [40].

5.2.1 Constant shaft speed mode

The constant shaft speed of the compressors is considered since different wind power output will affect the mass flow rate of compressed air which will have an impact on the pressure ratio and isentropic efficiency of the compressors (as shown in Figure 8) in the CAES charging process. For this case study, the wind power output condition within 24 hours has been presented in Table 8. The average value of wind power output for each hour was calculated based on the wind power output in Figure 3. The power demand is 110 MWe required from wind power output. The input parameters of the CAES system is listed in Table 5. The LPC and HPC operate at constant shaft speeds of 3000 rpm and 7620 rpm respectively and are connected by a gearbox. The different operating points from characteristic curves of the compressors and the turbines at design condition (refer to $v=1$ in Figures 4 (a) (b) and 5 (a) (b)) were used to obtain their corresponding performance data which is included in Aspen Plus[®] models through Performance Rating.

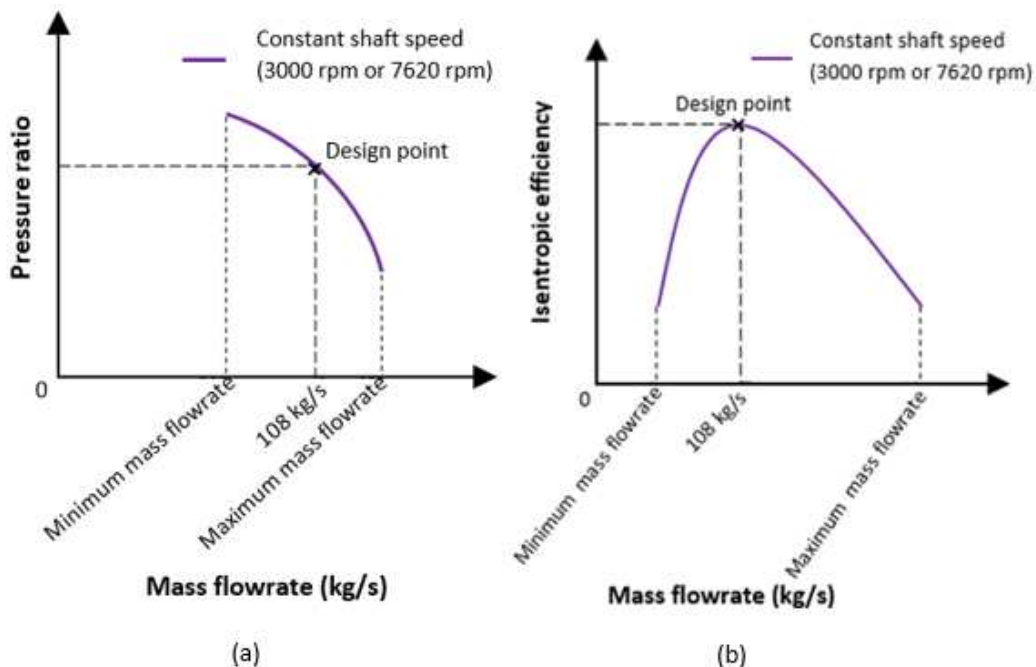


Figure 8. The sketch map of the relationship between both (a) pressure ratio and (b) isentropic efficiency with mass flowrate for LPC and HPC at constant shaft speed mode

Table 8. The condition of wind power output within 24 hours.

Time (Hour)	Wind power output (MW)	Excess or insufficient wind power (MW)
00:00:00	114.50	4.50
01:00:00	118.00	8.00
02:00:00	136.75	26.75
03:00:00	147.00	37.00
04:00:00	150.50	40.50
05:00:00	159.25	49.25
06:00:00	172.50	62.50
07:00:00	169.75	59.75
08:00:00	184.50	74.50
09:00:00	194.00	84.00
10:00:00	196.75	86.75
11:00:00	194.00	84.00
12:00:00	182.25	72.25
13:00:00	151.75	41.75
14:00:00	144.25	34.25
15:00:00	131.50	21.50
16:00:00	108.75	- 1.25
17:00:00	82.50	- 27.50
18:00:00	59.75	- 50.25
19:00:00	40.50	- 69.50
20:00:00	34.50	- 75.50
21:00:00	35.50	- 74.50
22:00:00	49.00	- 61.00
23:00:00	85.25	- 24.75

The simulation results of Figure 9 present that the mass flow rate changes with wind power and operation condition for charging and discharging processes of the CAES system for wind power at constant shaft speed mode. From the results, the charging process of the CAES system can utilise excess wind power to store compressed air for only 7 hours because the constant shaft speed of LPC limits the flow rate range of the compressed air to between 106.40 kg/s and 120.5 kg/s. If the flow rate is less than 106.4 kg/s, this could cause surge condition in the LPC. The flow rate in the charging

process also cannot exceed 108 kg/s due to the rated mass flow rate at design condition. This will result in a limitation in the utilisation range of electricity taken from wind power, the electricity taken from the wind power for driving the compressors will be limited to the range between 57.62 MW (106.40kg/s) and 60 MW (108 kg/s). In the discharging process, the constant shaft speed of the turbines limits flowrate range of the compressed air to be between 55.00 kg/s and 99.60 kg/s. Thus, the discharging power of the CAES system will be between 29.77 MW and 75.50 MW.

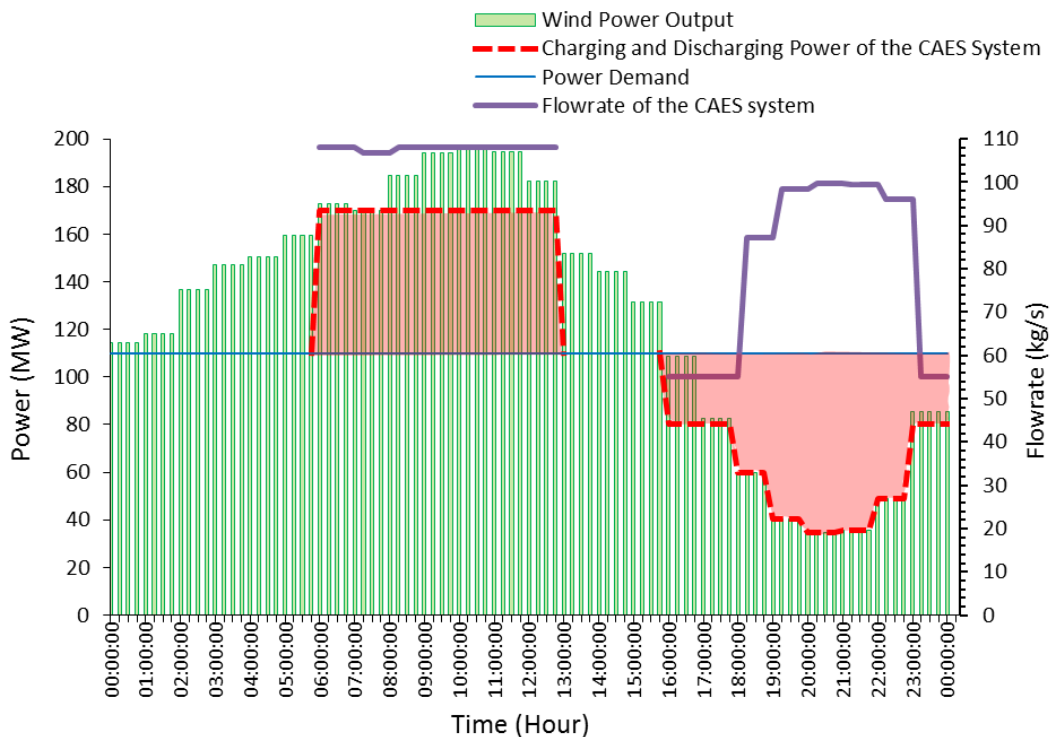


Figure 9. The simulation results and operation condition of the CAES system for wind power at constant shaft speed mode within 24 hours

As for the charging and discharging time, the charging process of the CAES system for wind power taken from excess wind power can be limited and operated from 6 am to 12 pm for 7 hours, the discharging process of the CAES system for generating electricity can be operated from 4 pm to 11 pm for 8 hours. Figure 10 indicates the mass change of compressed air and pressure change of the cavern. The pressure of the cavern is an important factor considered in the operation process of the CAES system for wind power because the pressure of the cavern should be kept at the range of the regular operation pressure in the charging and discharging processes. Additionally, the round-trip efficiency of the CAES system for wind power at the constant shaft speed mode is calculated to be 47.15%. After 24 hours operation in Figure 10, it is found that the remaining mass of compressed air

and the pressure of the cavern are still more and higher than the minimum operation requirement of the cavern. Therefore, the CAES system can continue to generate more electricity, which will improve the round-trip efficiency of the CAES system integrated with wind power from 47.15% to 50.98%.

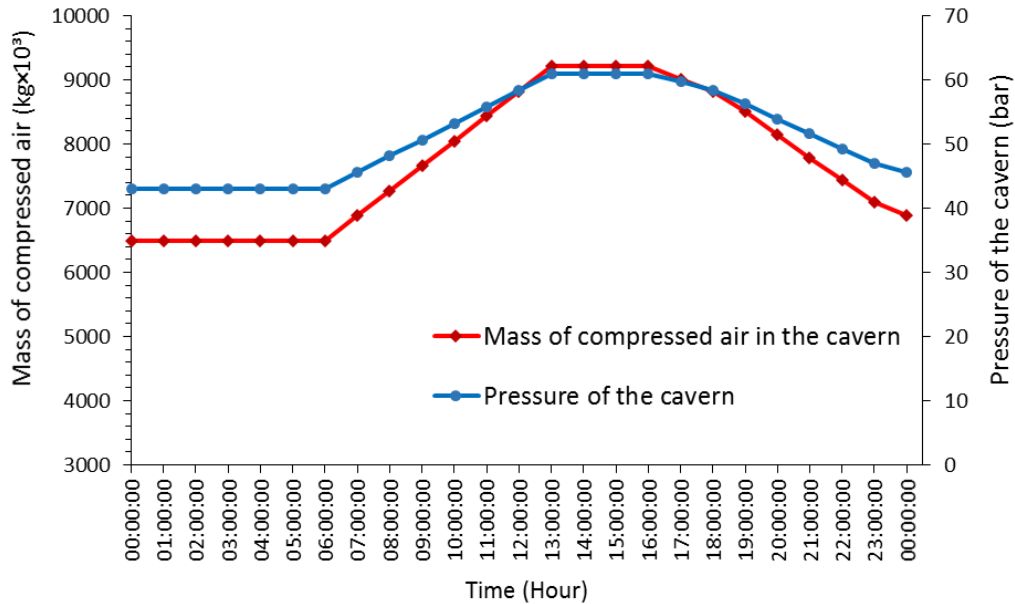


Figure 10. Mass of the compressed air and pressure in the cavern of the CAES system for wind power at constant shaft speed mode within 24 hours

5.2.2 Variable shaft speed mode

Variable shaft speed operation of the compressors should also be considered because the mass flow rate range was bounded at the constant shaft speed mode in Section 5.2.1. Also, the different wind power will affect the mass flow rate of compressed air which also has an impact on the pressure ratio and shaft speed of the LPC and HPC. Therefore, it is also essential to investigate the effect of variable shaft speed mode on the CAES system for wind power. For this case study, the wind power output condition is same with the previous section in Table 8. The input conditions of the CAES system were same as Section 5.2.1. The characteristic curves of the compressors were used to obtain their corresponding performance data, which followed the optimal efficiency line enable LPC and HPC to operate at optimal efficiency at different shaft speeds (as shown with the solid green line in Figure 4 (a) (b) ‘Optimal efficiency’).

From the simulation results of Figures 11 and 12, the mass flow rate changes with utilised excess wind power and operation condition for charging and discharging processes of the CAES system for fluctuating wind power and cavern condition were presented. Compare with the constant shaft speed mode, the CAES system for wind power at variable shaft speed mode can compress more mass of

compressed air for energy storage than that at constant shaft speed mode. The charging process of the CAES system can be operated at a wider range of flow rate between 41.5 kg/s (power requirement of compressors is 7.1 MW) and 108 kg/s (60 MW). However, it is noticed that the inlet pressure of the cavern (also the pressure after the aftercooler) through a throttle valve should be considered and this pressure should be higher than existing pressure of the cavern. Otherwise, the compressed air cannot be injected into the cavern. Therefore, the charging time of the CAES system taking excess wind power and ensuring the inlet pressure to be higher than the existing pressure of the cavern was from 5 am to 1 pm for 8 hours. As for the discharging process, the operation condition at variable shaft speed mode is same as that at constant shaft speed mode due to the same condition of both modes. The round-trip efficiency of the integrated system at variable shaft speed mode is calculated to be 44.68%. From Figure 12, it is also found that the remaining mass of compressed air and the pressure of the cavern are still more and higher than the minimum operation requirement of the cavern after 24 hours operation. Therefore, the system can continue to generate more electricity, which will improve the round-trip efficiency of the CAES system integrated with wind power from 44.68% to 51.69%.

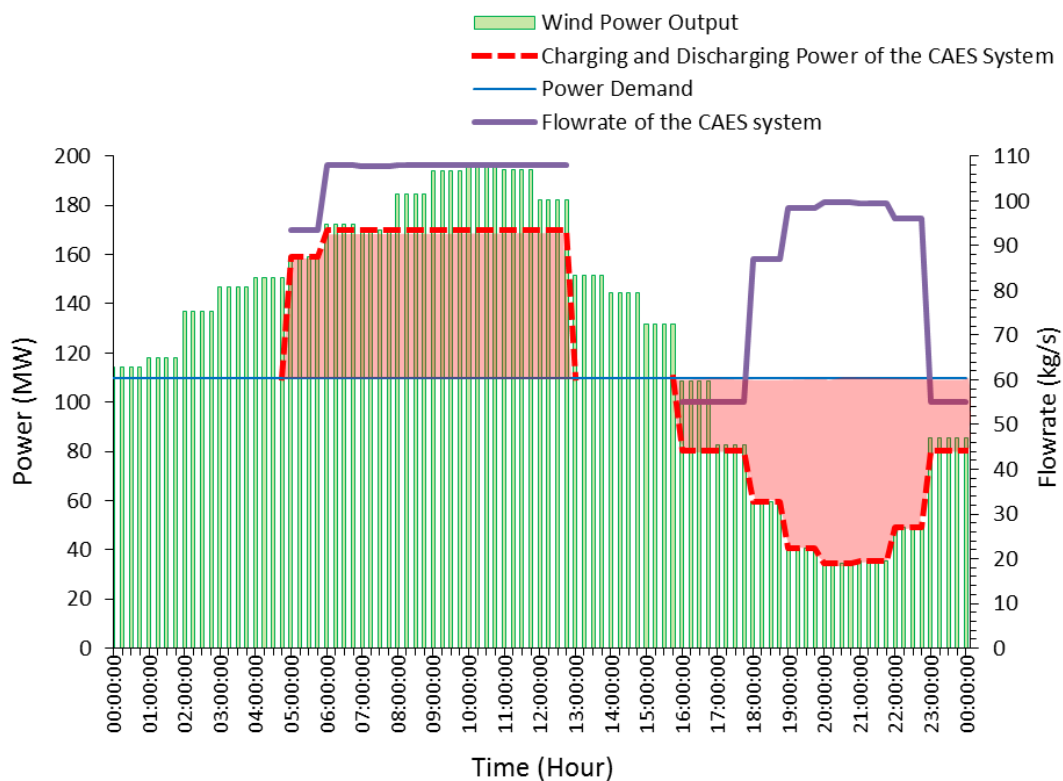


Figure 11. The simulation results and operation conditions of the CAES system for wind power at variable shaft speed mode within 24 hours

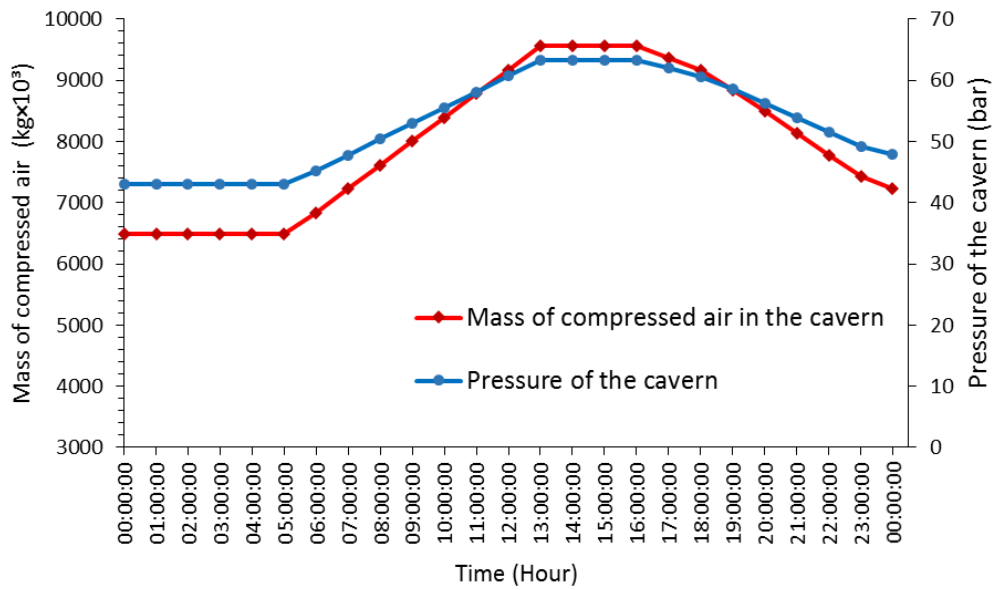


Figure 12. Mass of the compressed air and pressure in the cavern of the CAES system for wind power at variable shaft speed mode within 24 hours

5.2.3 Comparison between two modes

Comparing the design and off-design conditions, it is evident that the round-trip efficiency of the CAES system for wind power at design condition is higher than that at off-design conditions. The reason is that the CAES system for wind power can operate at optimal operating points at design condition. However, the CAES system for the fluctuating wind power operated at design condition can only be an ideal case.

Comparing both modes at off-design conditions, both modes have same electricity generation in the discharging process within 24 hours, but the charging process at variable shaft speed mode can utilise more excess wind energy for energy storage than at constant shaft speed mode. From the simulation results of Figures 9 and 11, the CAES system for wind power at variable shaft speed mode can use more excess wind energy (49.25 MWh) than constant shaft speed mode. From the remaining mass of compressed air and pressure of the cavern at both modes in Figures 10 and 12, the CAES system for wind power at variable shaft speed mode can store more compressed air (51.55×10^3 kg) in the cavern than that at constant shaft speed mode. When the discharging process of the CAES system for wind power at both modes continue to operate for generating electricity in discharging process after 24 hours, the integrated system at variable shaft speed mode can generate more electricity (76.00 MWh) and provide longer discharging time than that at constant shaft speed mode. In this case, when the mass of the compressed air in the cavern at both modes can be utilised until to the same minimum operation pressure of the cavern (43 bar), the round-trip efficiency of the CAES system integrated

with wind power at variable shaft speed mode (51.69%) is higher than that at constant shaft speed mode (50.98%). Moreover, the variable shaft speed compressor will save more electricity consumption than constant shaft speed compressor because the constant shaft speed compressor can only be very efficient when operating at design condition, it cannot change the shaft speed for lower mass flow rate. The variable shaft speed compressor can change the shaft speed with the different air mass flow rates, which can reduce energy consumption by about 35% [54]. Therefore, the CAES system for wind power at variable shaft speed mode could be better choice than constant shaft speed mode, due to higher round-trip efficiency, more utilisation of excess wind power and more power output.

6. Economic evaluation

6.1 Methodology

The economic evaluation was implemented in APEA V8.4. APEA is a professional and industrial standard engineering tool. It is considered to be more accurate than correlation-based economic evaluation methods [55]. APEA can be used for engineering design and evaluation of different types of projects because it includes design procedures and price data for many types of project materials and components, also it considers engineering contingency (5%). A bottom-up method is used by APEA. The unit operations were mapped to individual equipment cost model that can be designed manually because of some special components when the model was implemented in APEA.

The LCOE of the CAES system for wind power was calculated by dividing the total annual cost (TAC) by the annual net power output (E_{output}), as expressed in Equation (4) [56]. TAC is a sum of annualised capital expenditure (ACAPEX), fixed operation expenditure (FOPEX) and variable operational expenditure (VOPEX) described in Equation (5) [55–57]. CAPEX involves costs of equipment materials and installation, engineering and management, labour generated during plant construction. ACAPEX is the product of CAPEX and capital recovery factor (CRF), as written by Equations (6) and (7) [56,57]. FOPEX involves the costs of long term service agreement, operating and maintenance and other fixed costs which could be generated during the periods of full load or shutdown.

$$LCOE = \frac{TAC}{E_{output}} \quad (4)$$

$$TAC = ACAPEX + FOPEX + VOPEX \quad (5)$$

$$ACAPEX = CAPEX \times CRF \quad (6)$$

$$CRF = \frac{i(1+i)^n}{(1+i)^n - 1} \quad (7)$$

CRF is determined by n (specifying the CAES plant life) and i (discount rate). Capacity factor is the total time of power output expected in one year. Regarding to the aforementioned equations, a simplified model described in Equation (8) can be used to calculate the LCOE of the CAES system for wind power in [57]:

$$\text{LCOE} = \{(\text{CAPEX} \times \text{CRF} + \text{FOPEX}) / (365\text{days} \times 24\text{hours} \times \text{Capacity factor})\} + \text{Fuel cost/kWh} + \text{Electricity consumption cost/kWh} \quad (8)$$

As for the CAES system in the context of wind power, the investigation of the LCOE with different modes is important for comparing their economic advantages. The compressors of the charging process consume excess wind power to compress the air for storing energy in the cavern. It means that the CAES system can use free or cheaper electricity to compress air at the off-peak time. Some parameters given in Table 9 were implemented for the LCOE model.

Table 9. Parameters for LCOE model [57].

Parameters description	Value
CAES plant lifetime (years)	20
Discount rate (%)	4
CRF	0.074
Fuel cost (\$/Thousand Cubic Feet) [58]	3.426
Engineering contingency	5%

6.2 Comparison of the price at different conditions and different power sources

Table 10 presents the LCOE of the CAES system for wind power at design and off-design conditions. From the results, the LCOE of the CAES system for wind power at design condition (4.94 cents/kWh) is the cheapest of all. At off-design conditions, the LCOE of the CAES system for wind power within 24 hours is higher than that at the minimum operation pressure (43 bar) of the cavern because the stored compressed air was not fully discharged within 24 hours in this study and

the CAES system can continue to produce more electricity after 24 hours. When both modes were operated within 24 hours, the LCOE at constant shaft speed mode is cheaper than that at variable shaft speed mode. However, the LCOE at constant shaft speed mode is higher than that at variable shaft speed mode, when both modes were operated at a same operating pressure of the cavern with 43 bar. Moreover, the LCOEs at these three modes are lower than the residential electricity price (12.75 cents/kWh [59]).

Table 10. Comparison of costs of CAES system for wind power at design and off-design conditions

Variables (cents/kWh)	Design condition	Off-design conditions ^a		Off-design conditions ^b	
		Constant shaft speed mode ¹	Variable shaft speed mode ¹	Constant shaft speed mode ²	Variable shaft speed mode ²
ACAPEX	3.335	5.695	5.695	4.820	4.180
FOPEX	1.548	2.125	2.300	1.894	1.857
Fuel cost	0.058	0.0588	0.0588	0.0587	0.0586
LCOE	4.94	7.88	8.05	6.77	6.10

a. The CAES system for wind power was operated within only 24 hours of this study.

b. The CAES system for wind power was operated until to the minimum operation pressure (43 bar) of the cavern.

Figure 13 shows a comparison of LCOE between the CAES system and different types of power generation sources. The CAES system in the context of wind power can provide the price of electricity that could be cheaper than some renewable energies (e.g. offshore wind power and solar power), hydropower and nuclear power, even also some conventional power (Natural gas combustion turbine) [60,61]. The CAES system for the wind power is capable of balancing supply and demand of the grid. This function of the CAES system for wind power could have more potential value than the reasonable LCOE [57].

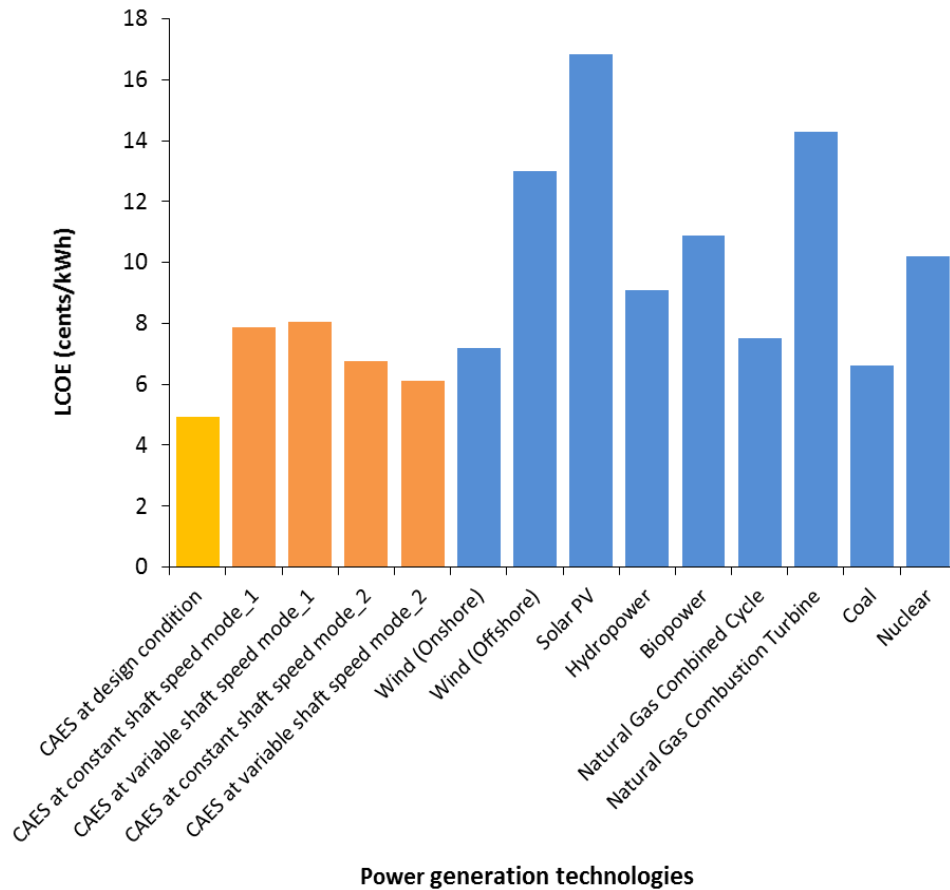


Figure 13. Comparative LCOE between the CAES system integrated with wind power and different power generation technologies [60,61]

7. Conclusions

In this study, the improved models for the compressors, turbines and the proposed CAES system in the context of wind power were developed in Aspen Plus[®] and a pseudo-dynamic model for the cavern was developed in Excel with input parameters based on industrial operation considerations. The performance investigation and economic evaluation at design conditions and off-design conditions were carried out. The main conclusions are summarised as follows:

- The CAES system for wind power at constant and variable shaft speed modes can utilise excess wind electricity to store the compressed air and it can expand compressed air to generate electricity to smooth the fluctuating wind power with proposed different operating strategies.
- In the process analysis of off-design conditions, the range of air mass flow rate in the charging process of the CAES system for wind power at constant shaft speed mode was limited, which results in a limitation of the utilisation range of electricity taken from wind power. The range

of air mass flow rate of the CAES system for wind power at variable shaft speed mode has a much wider range of the mass flow rate than that at constant shaft speed mode.

- The CAES system for wind power at variable shaft speed model has better performance than that at constant shaft speed. This is because the CAES system at variable shaft speed mode utilise more excess wind energy (49.25 MWh), store more compressed air (51.55×10^3 kg), generate more electricity (76.00 MWh) and provide longer discharging time than at constant shaft speed mode.
- The LCOE for the CAES system in the context of wind power at variable shaft speed mode is lower than that at constant shaft speed mode and the LCOE at both modes are lower than some renewable energies (e.g. offshore wind power and solar power), hydropower, nuclear power, some conventional powers (natural gas combustion turbine) and the residential electricity price. The CAES system could be an effective solution and promising approach for operating and utilising wind power for residential power supply flexibly.

References

- [1] Z. Pan, G. Lin, J. Wang, Y. Dai, Energy efficiency analysis and off-design analysis of two different discharge modes for compressed air energy storage system using axial turbines, *Renewable Energy*. 85 (2016) 1164–1177. doi:10.1016/J.RENENE.2015.07.095.
- [2] X. Liu, J. Chen, X. Luo, M. Wang, H. Meng, Study on heat integration of supercritical coal-fired power plant with post-combustion CO₂ capture process through process simulation, *Fuel*. 158 (2015) 625–633. doi:10.1016/j.fuel.2015.06.033.
- [3] E.A. Bouman, M.M. Øberg, E.G. Hertwich, Environmental impacts of balancing offshore wind power with compressed air energy storage (CAES), *Energy*. 95 (2016) 91–98. doi:10.1016/j.energy.2015.11.041.
- [4] W. Ji, Y. Zhou, Y. Sun, W. Zhang, B. An, J. Wang, Thermodynamic analysis of a novel hybrid wind-solar-compressed air energy storage system, *Energy Conversion and Management*. 142 (2017) 176–187. doi:10.1016/j.enconman.2017.02.053.
- [5] I. Arsie, V. Marano, G. Rizzo, M. Moran, Integration of wind turbines with compressed air energy storage, in: *AIP Conference Proceedings*, 2009: pp. 11–18.
- [6] H. Chen, T.N. Cong, W. Yang, C. Tan, Y. Li, Y. Ding, Progress in electrical energy storage system: A critical review, *Progress in Natural Science*. 19 (2009) 291–312. doi:10.1016/j.pnsc.2008.07.014.
- [7] M. Beaudin, H. Zareipour, A. Schellenberg, W. Rosehart, Energy Storage for Mitigating the Variability of Renewable Electricity Sources, in: *Energy Storage for Smart Grids: Planning and Operation for Renewable and Variable Energy Resources (VERs)*, 2014: pp. 1–33. doi:10.1016/B978-0-12-410491-4.00001-4.
- [8] Y. Liu, C.K. Woo, J. Zarnikau, Wind generation's effect on the ex post variable profit of compressed air energy storage: Evidence from Texas, *Journal of Energy Storage*. 9 (2017) 25–39. doi:10.1016/j.est.2016.11.004.
- [9] R. Sioshansi, P. Denholm, T. Jenkin, A comparative analysis of the value of pure and hybrid electricity storage, *Energy Economics*. 33 (2011) 56–66. doi:10.1016/j.eneco.2010.06.004.
- [10] H. Chen, C. Tan, J. Liu, X. Zhang, Compressed air energy storage, in: *Energy Storage - Technologies and Applications*, INTECH, 2013: pp. 101–112.
- [11] X. Luo, J. Wang, M. Dooner, J. Clarke, Overview of current development in electrical energy storage technologies and the application potential in power system operation, *Applied Energy*. 137 (2015) 511–536. doi:10.1016/j.apenergy.2014.09.081.
- [12] H. Ibrahim, A. Ilinca, J. Perron, Energy storage systems—Characteristics and comparisons, *Renewable and Sustainable Energy Reviews*. 12 (2008) 1221–1250. doi:10.1016/j.rser.2007.01.023.
- [13] J. Radcliffe, Energy storage technologies, *Ingenia*. (2013) Issue 54: 27–32.
- [14] F. Díaz-González, A. Sumper, O. Gomis-Bellmunt, R. Villafáfila-Robles, A review of energy storage technologies for wind power applications, *Renewable and Sustainable Energy Reviews*. 16 (2012) 2154–2171. doi:10.1016/j.rser.2012.01.029.
- [15] T. Kousksou, P. Bruel, A. Jamil, T. El Rhafiki, Y. Zeraoui, Energy storage: Applications and challenges, *Solar Energy Materials and Solar Cells*. 120 (2014) 59–80.

doi:10.1016/j.solmat.2013.08.015.

- [16] M. Aneke, M. Wang, Energy storage technologies and real life applications – A state of the art review, *Applied Energy*. 179 (2016) 350–377. doi:10.1016/j.apenergy.2016.06.097.
- [17] P. Denholm, G.L. Kulcinski, Life cycle energy requirements and greenhouse gas emissions from large scale energy storage systems, *Energy Conversion and Management*. 45 (2004) 2153–2172. doi:10.1016/j.enconman.2003.10.014.
- [18] P. Denholm, T. Holloway, Improved accounting of emissions from utility energy storage system operation, *Environmental Science & Technology*. 39 (2005) 9016–9022.
- [19] H. Meng, M. Wang, M. Aneke, X. Luo, O. Olumayegun, X. Liu, Technical performance analysis and economic evaluation of a compressed air energy storage system integrated with an organic Rankine cycle, *Fuel*. 211 (2018) 318–330. doi:https://doi.org/10.1016/j.fuel.2017.09.042.
- [20] X. Luo, J. Wang, M. Dooner, J. Clarke, C. Krupke, Overview of Current Development in Compressed Air Energy Storage Technology, *Energy Procedia*. 62 (2014) 603–611. doi:10.1016/j.egypro.2014.12.423.
- [21] F. Crotonogino, K.-U. Mohmeyer, R. Scharf, Huntorf CAES: More than 20 years of successful operation, Orlando, Florida, USA. (2001).
- [22] C.A. of S. Energy Storage R&D Center, 10MW advanced compressed air energy storage system, (2016). <http://english.iet.cas.cn/Institute/6/> (accessed February 1, 2018).
- [23] Y. Zhang, Y. Xu, X. Zhou, H. Guo, X. Zhang, H. Chen, Compressed air energy storage system with variable configuration for wind power generation, *Energy Procedia*. 142 (2017) 3356–3362. doi:10.1016/J.EGYPRO.2017.12.470.
- [24] S. Simpure, F. Garde, M. David, O. Marc, J. Castaing-Lasvignottes, Design and Dynamic Simulation of a compressed Air Energy Storage System (CAES) Coupled with a Building, an Electric Grid and Photovoltaic Power Plant, in: CLIMA 2016, Aalborg, Denmark, 2016.
- [25] M.H. Balali, N. Nouri, A. Nasiri, H. Seifoddini, Development of an economical model for a hybrid system of grid, PV and Energy Storage Systems, in: 2015 International Conference on Renewable Energy Research and Applications (ICRERA), 2015: pp. 1108–1113. doi:10.1109/ICRERA.2015.7418582.
- [26] A.H. Alami, K. Aokal, J. Abed, M. Alhemyari, Low pressure, modular compressed air energy storage (CAES) system for wind energy storage applications, *Renewable Energy*. 106 (2017) 201–211. doi:10.1016/J.RENENE.2017.01.002.
- [27] A. Cavallo, Controllable and affordable utility-scale electricity from intermittent wind resources and compressed air energy storage (CAES), *Energy*. 32 (2007) 120–127. doi:10.1016/j.energy.2006.03.018.
- [28] V. Marano, G. Rizzo, F.A. Tiano, Application of dynamic programming to the optimal management of a hybrid power plant with wind turbines, photovoltaic panels and compressed air energy storage, *Applied Energy*. 97 (2012) 849–859. doi:10.1016/j.apenergy.2011.12.086.
- [29] S. Kahrobaee, S. Asgarpour, Optimum Planning and Operation of Compressed Air Energy Storage with Wind Energy Integration, in: North American Power Symposium (NAPS), 2013: pp. 1–6. doi:10.1109/NAPS.2013.6666909.

- [30] N.S. Hasan, M.Y. Hassan, M.S. Majid, H.A. Rahman, Mathematical Model of Compressed Air Energy Storage in Smoothing 2MW Wind Turbine, in: Power Engineering and Optimization Conference, 2012: pp. 339–343. doi:10.1109/PEOCO.2012.6230886.
- [31] D. Lobera, A. Foley, Modelling gas storage with compressed air energy storage in a system with large wind penetrations, in: 7th Conference on Sustainable Development of Energy, Water and Environment Systems, 2012: pp. 1–13.
- [32] M. Saadat, F.A. Shirazi, P.Y. Li, Modeling and control of an open accumulator Compressed Air Energy Storage (CAES) system for wind turbines, *Applied Energy*. 137 (2015) 603–616. doi:10.1016/j.apenergy.2014.09.085.
- [33] S. Briola, P. Di Marco, R. Gabbrielli, J. Riccardi, A novel mathematical model for the performance assessment of diabatic compressed air energy storage systems including the turbomachinery characteristic curves, *Applied Energy*. 178 (2016) 758–772. doi:10.1016/j.apenergy.2016.06.091.
- [34] H. Sun, X. Luo, J. Wang, Feasibility study of a hybrid wind turbine system–Integration with compressed air energy storage, *Applied Energy*. 137 (2015) 617–628.
- [35] C. Krupke, J. Wang, J. Clarke, X. Luo, Modeling and Experimental Study of a Wind Turbine System in Hybrid Connection With Compressed Air Energy Storage, *IEEE Transactions on Energy Conversion*. 32 (2017) 137–145. doi:10.1109/TEC.2016.2594285.
- [36] S. Li, Y. Dai, Design and Simulation Analysis of a Small-Scale Compressed Air Energy Storage System Directly Driven by Vertical Axis Wind Turbine for Isolated Areas, *Journal of Energy Engineering*. 141 (2015) 1–11. doi:10.1061/(ASCE)EY.1943-7897.0000207.
- [37] H. Ibrahim, R. Younès, A. Ilinca, M. Dimitrova, J. Perron, Study and design of a hybrid wind-diesel-compressed air energy storage system for remote areas, *Applied Energy*. 87 (2010) 1749–1762. doi:10.1016/j.apenergy.2009.10.017.
- [38] M.A. Riaz, Feasibility of compressed air energy storage to store wind on monthly and daily basis, Iowa State University, 2010. <http://lib.dr.iastate.edu/etd/11722> (accessed May 30, 2018).
- [39] J. Wang, K. Lu, L. Ma, J. Wang, M. Dooner, S. Miao, J. Li, D. Wang, Overview of Compressed Air Energy Storage and Technology Development, *Energies*. 10 (2017). doi:10.3390/en10070991.
- [40] H. Hoffeins, Huntorf air storage gas turbine power plant, *Energy Supply, Brown Boveri Publication DGK*. 90 (1994) 1–14.
- [41] EnggCyclopedia, Axial and centrifugal-type compressors, (2012). <http://www.enggcyclopedia.com/2012/03/axial-centrifugal-type-compressors/> (accessed May 30, 2018).
- [42] F. Kraftwerk, The difference between steam and gas turbines, (2018). <http://kraftwerkforschung.info/en/quickinfo/basic-concepts/the-difference-between-steam-and-gas-turbines/> (accessed May 30, 2018).
- [43] F.S. Barnes, J.G. Levine, Compressed Air Energy Storage, in: *Large Energy Storage Systems Handbook*, CRC Press, Boca Raton, 2011.
- [44] EIRGRID GROUP, Northern Ireland - Actual and Forecast Wind, (2017). <http://www.eirgridgroup.com/how-the-grid-works/system-information/> (accessed June 7,

2017).

- [45] B.M. Enis, P. Lieberman, I. Rubin, Operation of Hybrid Wind-Turbine Compressed-Air System for Connection to Electric Grid Networks and Cogeneration, *Wind Engineering*. 27 (2003) 449–459. doi:10.1260/030952403773617436.
- [46] B.E. Poling, J.M. Prausnitz, J.P. O'Connell, N. York, C. San, F. Lisbon, L. Madrid, M. City, M. New, D. San, J.S. Singapore, S. Toronto, *THE PROPERTIES OF GASES AND LIQUIDS* McGRAW-HILL, 2001.
- [47] M. Nakashima, H. Kato, E. Takaoka, Development of real-time pseudo dynamic testing, *Earthquake Engineering & Structural Dynamics*. 21 (1992) 79–92. doi:10.1002/eqe.4290210106.
- [48] The Engineering Toolbox, Ideal Gas Law, (2018). https://www.engineeringtoolbox.com/ideal-gas-law-d_157.html (accessed November 26, 2018).
- [49] W. Liu, L. Liu, L. Zhou, J. Huang, Y. Zhang, G. Xu, Y. Yang, Analysis and optimization of a compressed air energy storage—combined cycle system, *Entropy*. 16 (2014) 3103–3120.
- [50] M. Budt, D. Wolf, R. Span, J. Yan, A review on compressed air energy storage: Basic principles, past milestones and recent developments, *Applied Energy*. 170 (2016) 250–268. doi:10.1016/j.apenergy.2016.02.108.
- [51] B. Elmegaard, W. Brix, Efficiency of compressed air energy storage, in: *24th International Conference on Efficiency, Cost, Optimization, Simulation and Environmental Impact of Energy Systems*, 2011.
- [52] A. Mohammadi, M.H. Ahmadi, M. Bidi, F. Joda, A. Valero, S. Uson, Exergy analysis of a Combined Cooling, Heating and Power system integrated with wind turbine and compressed air energy storage system, *Energy Conversion and Management*. 131 (2017) 69–78. doi:10.1016/j.enconman.2016.11.003.
- [53] K. Cen, Y. Chi, J. Yan, *Challenges of power engineering and environment: proceedings of the International Conference on Power Engineering 2007*, Springer Science & Business Media, 2009.
- [54] Atlas Copco, So many types of air compressor. What's the difference?, Atlas Copco. (2018). <https://www.atlascopco.com/en-uk/compressors/compressed-air-tips/types-of-air-compressors> (accessed September 15, 2018).
- [55] X. Luo, M. Wang, E. Oko, C. Okezue, Simulation-based techno-economic evaluation for optimal design of CO₂ transport pipeline network, *Applied Energy*. 132 (2014) 610–620. doi:10.1016/j.apenergy.2014.07.063.
- [56] X. Luo, M. Wang, Study of solvent-based carbon capture for cargo ships through process modelling and simulation, *Applied Energy*. 195 (2017) 402–413.
- [57] B.P. McGrail, J.E. Cabe, C.L. Davidson, F.S. Knudsen, D.H. Bacon, M.D. Bearden, M.A. Charmness, J.A. Horner, S.P. Reidel, H.T. Schaefer, F.A. Spane, P.D. Thorne, *Technoeconomic Performance Evaluation of Compressed Air Energy Storage in the Pacific Northwest*, Washington, 2013.
- [58] UEI, NATURAL GAS, Administration, U.S Energy Information. (2016). <https://www.eia.gov/dnav/ng/hist/n3035us3M.htm> (accessed January 20, 2017).

- [59] EIA, Electric Power Monthly, U.S. Energy Information Administration. (2016). https://www.eia.gov/electricity/monthly/epm_table_grapher.cfm?t=epmt_5_6_a (accessed January 20, 2017).
- [60] OpenEI, Transparent Cost Database, (2015). <http://en.openei.org/apps/TCDB/#blank> (accessed May 10, 2018).
- [61] LAZARD, LAZARD's levelized cost of energy analysis — version 8.0, (2014). https://www.lazard.com/media/1777/levelized_cost_of_energy_-_version_80.pdf (accessed April 20, 2018).